The Astrophysical Journal Letters, 942:L31 (6pp), 2023 January 10 https://doi.org/10.3847/2041-8213/acab50

Prospects for the Observation of Continuous Gravitational Waves from Spinning Neutron Stars Lensed by the Galactic Supermassive Black Hole

Soummyadip Basak[1,3], Aditya Kumar Sharma[1,3], Shasvath J. Kapadia[1], and Parameswaran Ajith[1,2]
[1] International Centre for Theoretical Sciences, Tata Institute of Fundamental Research, Bangalore 560089, India; aditya.sharma@icts.res.in
[2] Canadian Institute for Advanced Research, CIFAR Azrieli Global Scholar, MaRS Centre, West Tower, 661 University Ave, Toronto, ON M5G 1M1, Canada
Received 2022 May 11; revised 2022 December 13; accepted 2022 December 13; published 2023 January 11

Abstract

We study the prospects of detecting continuous gravitational waves (CGWs) from spinning neutron stars (NSs), gravitationally lensed by the galactic supermassive black hole. Assuming various astrophysically motivated spatial distributions of galactic NSs, we find that CGW signals from a few (∼0–6) neutron stars should be strongly lensed. Lensing will produce two copies of the signal (with time delays of seconds to minutes) that will interfere with each other. The relative motion of the NS with respect to the lensing optical axis will change the interference pattern, which will help us to identify a lensed signal. Accounting for the magnifications and time delays of the lensed signals, we investigate their detectability by ground-based detectors. Modeling the spin distribution of NSs based on that of known pulsars and assuming an ellipticity of $\epsilon = 10^{-7}$, lensed CGWs are unlikely to be detectable by LIGO and Virgo in realistic searches involving $\mathcal{O}(10^{12})$ templates. However, third-generation detectors have a ∼2%–51% probability of detecting at least one lensed CGW signal. For an ellipticity of $\epsilon = 10^{-8}$, the detection probability reduces to ∼0%–18%. Though rare, such an observation will enable interesting probes of the supermassive black hole and its environment.

Unified Astronomy Thesaurus concepts: Strong gravitational lensing (1643); Gravitational waves (678); General relativity (641); Gravitational wave astronomy (675); Gravitational wave sources (677); Neutron stars (1108)

1. Introduction

LIGO and Virgo detectors (Aasi et al. 2015; Acernese et al. 2015) have detected ∼100 transient gravitational-wave (GW) signals during their first three observing runs (Abbott et al. 2020a, 2021), most of which are consistent with GWs produced by coalescing binary black holes (BBHs). GWs from merging binary neutron stars (Abbott et al. 2017a, 2020) and neutron star–black hole binaries (Abbott et al. 2021a) have also been observed. These detections have afforded a plethora of scientific riches, including an unprecedented probe of the population of compact binaries (Abbott et al. 2021b), a distance-ladder-independent measurement of the Hubble constant (Abbott et al. 2017b), as well as some of the most stringent tests of Einstein's general theory of relativity in the strong-field regime (Abbott et al. 2020b).

Although there has so far been no confident detection of the gravitational lensing of GWs (Abbott et al. 2021c),[4] there is a growing consensus in the literature that lensed GWs from merging BBHs are likely to be detected in the upcoming observing runs of LIGO, Virgo, and KAGRA (see, e.g., Akutsu et al. 2021; Ng et al. 2018). Observations of such events will provide additional insights into various aspects of astrophysics, cosmology, and fundamental physics. Apart from being the very first detection of gravitational lensing involving a new messenger, they will enable accurate localization of the host galaxy of the merger (Hannuksela et al. 2020), provide unique constraints on the constituents of dark matter (Jung & Shin 2019; Urrutia & Vaskonen 2022; Basak et al. 2022), on models of the populations of galaxies and galaxy clusters (Smith et al. 2019), as well as on alternative theories of gravity (Fan et al. 2017; Ezquiaga & Zumalacárregui 2020; Goyal et al.2021).

While the list of detections of transient GWs has been growing from one observing run to the next (Abbott et al. 2019a, 2020a), and is expected to grow even more drastically in the future (Abbott et al. 2020), continuous GWs (CGWs) remain undetected (Abbott et al. 2019b, 2021d). Rapidly spinning, nonaxisymmetric neutron stars (NSs) in our galaxy are expected to produce CGWs potentially observable by ground-based detectors (see, e.g., Bonazzola & Gourgoulhon 1996).

In this Letter, we explore the prospects of observing the gravitational lensing of CGWs from spinning NSs by the galactic supermassive black hole (SMBH; Schödel et al. 2002; Ghez et al. 2003). Such an observation will provide potentially powerful probes of the properties of the astrophysical source as well as the lens. Focusing exclusively on strong lensing, we expect the CGWs to be lensed if the source NS resides within the Einstein angle of the lens. Assuming the SMBH to be a point-mass lens, strong lensing will produce two copies of a CGW, with a time delay between them.[5] The copies will have differing amplitudes, although their time-dependent phase will be identical. The image waveforms will show up in the detector as one superposed CGW, whose amplitude will depend on the magnifications of the images as well as the time delay between the two copies of the signal at the detector.

The number of NSs that are expected to lie within the Einstein angle of the SMBH will depend on the (poorly known)

[3] Equal contribution from both authors.
[4] Note, however, that some tantalizing candidates of lensed GW signals have been proposed; see, e.g., Dai et al. (2020).
[5] CGWs from rapidly spinning NSs, with spin frequencies spanning ∼100–1000 Hz, have wavelengths that are $\mathcal{O}(10^3$–$10^4)$ times smaller than the Schwarzschild radius of the galactic SMBH. The geometric optics approximation therefore holds for the lensing scenario considered here.

spatial distribution of NSs in the galaxy. We consider various astrophysically motivated distributions presented in the literature and evaluate the distribution of the number of NSs that fall within the Einstein angle, assuming a total of 10^9 NSs in the galaxy (Treves et al. 2000). We find that up to six NSs will be within the Einstein angle of the SMBH, so that their CGWs, if detected, will be strongly lensed.

We further assess the detectability of these signals by a third-generation (3G) GW detector network consisting of two Cosmic Explorers (CE; Evans et al. 2021) and one Einstein Telescope (ET; Punturo et al. 2010), incorporating the effects of lensing magnification and time delays. The detectability, characterized by the signal-to-noise ratio (S/N), is proportional to their amplitude, as well as the square root of the observation time (Jaranowski et al. 1998). The amplitude, in turn, is proportional to the ellipticity, the moment of inertia, and the square of the spin frequency of the NS (apart from extrinsic parameters such as the location and orientation).

We assume an ellipticity of 10^{-7}, which is one order of magnitude smaller than the best upper limits obtained from a directed search for NSs in the galactic center, for a fiducial moment of inertia of $10^{38}\,\mathrm{kg\,m^2}$ (Abbott et al. 2022). Spin frequencies are drawn from the spin distribution of known pulsars (Manchester et al. 2005). The signal amplitude is averaged over the inclination angle of the NS rotation axis with respect to the line of sight, over the angle between the rotation axis and the axis of symmetry, as well as the polarization angle. Using a single-template search (i.e., assuming that the source parameters are known a priori) the probability of detecting at least one lensed CGW signal is ∼0%–15% (2%–53%) in LIGO–Virgo (3G detectors). For a more realistic, directed search toward the galactic center using $\sim 10^{12}$ templates (Aasi et al. 2013), the corresponding probability is ∼0%–2% (2%–51%). Note that the ellipticity of most neutron stars could be much lower. For a more conservative assumption of $\epsilon = 10^{-8}$, LIGO–Virgo detectors are unlikely to detect any lensed signals. In 3G detectors, the detection probability is ∼1%–36% (∼0%–18%) for a single-template search (a directed search involving 10^{12} templates). If the ellipticity is lower than 10^{-8}, the detection probability will be even smaller.

A possible detection will enable very interesting probes of the physics and astrophysics of the source as well as the lens. The lensed CGW signal will contain imprints of the properties of the SMBH, such as its mass and spin, enabling an independent measurement of these properties. Such an observation might also enable us to constrain the presence of additional hairs of the black hole, thus probing the true nature of the supermassive compact object at the galactic center. In addition, stars and stellar-mass compact objects in the galactic center can cause additional microlensing effects on the CGW signal (e.g., Liao et al. 2019; Suvorov 2022). This will potentially allow us to probe the poorly understood astrophysical environment of the galactic center. Any proper motion of the NS will also leave an imprint in the CGW signal.

The rest of the Letter is organized as follows. Section 2 briefly introduces gravitational lensing by a point-mass lens. Section 3 describes the spatial distributions of NSs assumed, as well as the resulting estimate on the number of NSs strongly lensed by the galactic SMBH. Section 4 delineates the calculation of the S/N and provides the (S/N-threshold-dependent) probability of detecting a lensed CGW in the 3G era. Section 5 summarizes the Letter, discusses a potential means of identifying lensed CGW candidates, and the possible astrophysical measurements that can be performed from such an observation.

2. Gravitational Lensing by a Point-mass Lens

The strong lensing of GWs, in the geometric optics limit, is identical to that of the lensing of electromagnetic waves and applies in general to null geodesics (see, e.g., Dodelson 2017). Thus, as with the gravitational lensing of light, the fundamental equation that governs strong lensing of GWs is the so-called lens equation that relates the source location $\vec{\beta}$, with the image location $\vec{\theta}$, via a deflection angle $\vec{\alpha}(\vec{\theta})$:

$$\vec{\beta} = \vec{\theta} - \vec{\alpha}(\vec{\theta}). \tag{1}$$

Note that $\vec{\beta}$, $\vec{\theta}$ are angles measured with respect to the line connecting the Earth and the lens, called the optical axis. The deflection angle $\vec{\alpha}(\vec{\theta})$ depends on the relative locations of the Earth, the lens, and the source, as well as the gravitational potential of the lens. For a point-mass lens with mass M_L,

$$\vec{\alpha} = \frac{\theta_E^2}{\theta^2}\vec{\theta}, \tag{2}$$

where θ_E is the Einstein angle (Einstein radius). In terms of the Schwarzschild radius $R_s = 2GM_L/c^2$ of the lens, this angle can be written as

$$\theta_E = \sqrt{\frac{2R_s D_{SL}}{D_S D_L}}. \tag{3}$$

Here, D_S and D_L are the distances (from Earth) to the source and the lens, respectively, and $D_{SL} = D_S - D_L$.[6] Multiple images are produced when the source is within the Einstein angle of the lens. This is a conservative assumption, as in the case of a point mass lens, multiple images can be produced even when the source is outside the Einstein radius. Solving the lens equation with the deflection angle for a point-mass lens yields two images at locations

$$\theta_\pm = \frac{\beta}{2}\left[1 \pm \sqrt{1 + \frac{4\theta_E^2}{\beta^2}}\right]. \tag{4}$$

The magnifications of the images can be acquired from the inverse of the determinant of the Jacobian transformation matrix between $\vec{\beta}$ and $\vec{\theta}$:

$$\mu = \det\left(\frac{\partial\vec{\beta}}{\partial\vec{\theta}}\right)^{-1}. \tag{5}$$

For a point-mass lens, the magnifications of the two images reduces to

$$\mu_\pm = \left[1 - \left(\frac{\theta_E}{\theta_\pm}\right)^4\right]^{-1}. \tag{6}$$

The time delay in the arrival of the two images at Earth has two contributing pieces. There is a geometric time delay due to the different paths traveled by the rays pertaining to each of the

[6] Since the distances considered in this work are galactic, cosmological effects are negligible. These distances can therefore be approximated to be Euclidean.

images. There is also a Shapiro time delay, caused by the general relativistic time dilation suffered by the rays when they venture into the vicinity of the lens. For a point-mass lens, the total time delay for sources that lie within the Einstein angle is to a good approximation given by

$$\Delta t \simeq 2\frac{D_{\rm L}D_{\rm S}}{cD_{\rm SL}}\theta_E\beta. \tag{7}$$

3. Number of Strongly Lensed Neutron Stars

Investigating the prospects of detecting lensed CGWs involves counting the expected number of NSs within the Einstein angle of the SMBH and assessing the detectability of CGWs produced by them. This requires assumptions on the total number of NSs in our galaxy and their spatial distribution. While it is generally believed that $\sim 10^9$ NSs reside in our galaxy, only $\sim 10^3$ have been detected so far through electromagnetic observations. Thus, little is known about the statistical properties of galactic neutron stars, including their spatial distribution.

We consider three types of spatial distribution of NSs in the galaxy. One assumes that NSs have the same distribution of stars in the young galactic disk. Following Paczynski (1990), we write the probability distributions in galactocentric cylindrical coordinates system (R, ϕ, z), where the z-axis corresponds to the rotation axis of the Milky Way, as

$$\frac{dP}{dR} = a_R\,\frac{R}{R_0^2}\exp\left(\frac{-R}{R_0}\right), \tag{8}$$

$$\frac{dP}{dz} = \frac{1}{2z_0}\exp\left(\frac{-|z|}{z_0}\right), \tag{9}$$

where $R_0 = 4.5$ kpc and $z_0 = 0.07$ kpc are scaling constants. We call this the "progenitor" model.

This will be a good approximation of the spatial distribution of the NSs if their natal kicks are small or when the NSs are young. However, the distribution of NSs can differ from that of stars depending on the NS birth velocities, which remains largely uncertain. To mimic the effect of natal kicks on the spatial distribution of NSs, some authors have considered different choices of z_0 in Equation (9). For example, Reed et al. (2021) use a range of z_0 values out of which we choose four different values ($z_0 = 0.1$, 0.2, 0.5, 1 kpc) in Equation (9) along with a Gaussian-like distribution in R:

$$\frac{dP}{dR} = \frac{R}{\sigma_{\rm R}^2}\exp\left(\frac{-R^2}{2\sigma_{\rm R}^2}\right), \tag{10}$$

where $\sigma_{\rm R} = 5$ kpc. Several studies also have evolved populations of NSs in the galactic potential by considering different models of the birth velocity to predict the expected distribution of NSs in the present epoch. Sartore et al. (2010) assume that the NSs are born in the galaxy with a constant birth rate, at locations given by the progenitor distribution presented in Equations (8)–(9). They evolved this distribution under several different assumptions on their birth velocities (indicated by A, B, C, D, and E) and two different models of the galactic potential (models with and without an asterisk). By fitting their simulation data, Sartore et al. (2010) presented the following

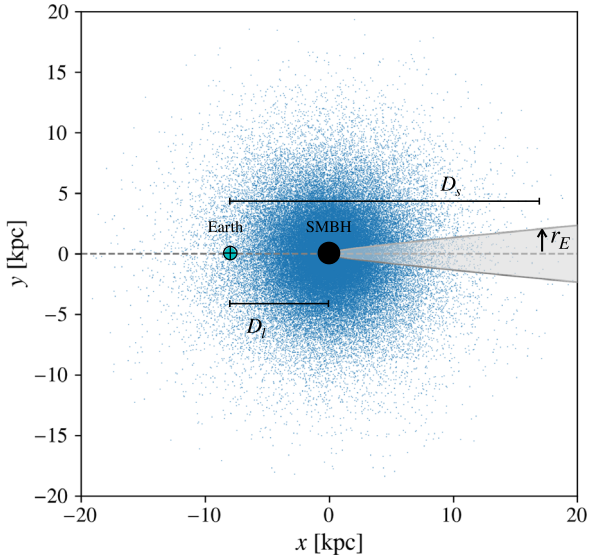

Figure 1. Schematic diagram of the distribution of neutron stars (blue dots) projected onto our galactic plane. The Einstein cone of the central SMBH is shown by the gray region (highly exaggerated). The neutron stars within the Einstein cone will be strongly lensed by the SMBH.

fitting functions:

$$\frac{dP}{dR} \propto R\exp\left(a_0 + a_1R + a_2R^2 + a_3R^3 + a_4R^4\right), \tag{11}$$

$$\frac{dP}{dz} \propto \frac{1}{b_0 b_1^{z} + b_2}, \tag{12}$$

where the fitting coefficients are tabulated in Tables A.1 and A.2 of Sartore et al. (2010).

For all models, we finally construct the three-dimensional distribution

$$\frac{dP}{dRd\phi dz} = C\,\frac{dP}{dR}\,\frac{dP}{d\phi}\,\frac{dP}{dz}, \tag{13}$$

where all models assume axial symmetry around the rotation axis of the galaxy ($dP/d\phi = 1/2\pi$). The distributions in Paczynski (1990) and Reed et al. (2021) are already normalized; hence, $C = 1$. For Sartore et al. (2010) models, the normalization constant C is determined by the condition that a certain fraction of the NSs presently resides in the disk of the galaxy:

$$\int_{R=0}^{R_{\rm disk}} dR \int_{\phi=0}^{2\pi} d\phi \int_{z=-z_{\rm disk}}^{z_{\rm disk}} dz \frac{dP}{dRd\phi dz} = f_{\rm disk}. \tag{14}$$

Above, $R_{\rm disk} = 20$ kpc and $z_{\rm disk} = 0.2$ kpc, while $f_{\rm disk}$ is given in Table 4 of Sartore et al. (2010).

In order to find the average number of NSs that would be strongly lensed (producing multiple images), we integrate the probability $dP/dRd\phi dz$ over a cone-like region around the optical axis with a radius of $r_E \equiv \theta_E D_s$ (shaded region Figure 1) and multiply it with the total expected number of NSs in the galaxy ($N \sim 10^9$):

$$\bar{N}_{\theta_E} = N\int_{\rm lensing\ cone} dRd\phi dz \frac{dP}{dRd\phi dz}. \tag{15}$$

Depending on the distribution $\bar{N}_{\theta_E}$ varies from 0.1 to 5.6. Assuming no spatial clustering of NSs, the actual number, N_{θ_E},

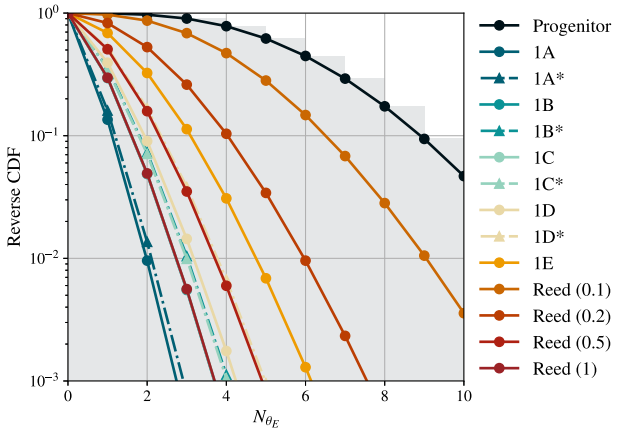

Figure 2. Cumulative distribution of the expected number of NSs within the Einstein angle of the galactic SMBH as predicted by different models of the NS spatial distribution and galactic potential. "Progenitor" model assumes that the spatial distribution of NSs follows that of the stars in the galaxy (Paczynski 1990). Models 1A, 1B, 1C, 1D, and 1E are predicted by Sartore et al. (2010) assuming different models of NS birth velocities. The dashed curves correspond to models 1A*, 1B*, 1C*, and 1D* of Sartore et al. (2010), which assume the same NS birth velocities but a different model for the galactic potential. For the Reed et al. (2021) models, we consider different values of z_0 (shown in brackets, in kpc). The probability of at least one NS being inside the lensing cone, $P(N_{\theta_E} \geqslant 1)$, is ∼0.1–1, depending on the model.

of NSs that will be strongly lensed by the SMBH will be distributed according to a Poisson distribution with mean $\bar{N}_{\theta_E}$. Figure 2 shows the distribution of N_{θ_E} for various models of the NS spatial distribution and galactic potential. We see that the probability of at least one NS being inside the lensing cone is significant ∼0.1–1, depending on the model).

4. Lensed Continuous GWs and Their Detectability

In order to assess the detectability of lensed CGWs, we need to compute their S/N at the detector. We model the NS as a triaxial ellipsoid (see, e.g., Andersson 2019). Its ellipticity is defined in terms of the moments of inertia around the rotation axis (I) and in the plane perpendicular to the principal axis (I_1, I_2):

$$\epsilon = \frac{|I_1 - I_2|}{I}. \tag{16}$$

If the rotation axis of the spinning NS does not align with the principal axis, the resulting time-varying mass quadrupole moment will produce GWs whose amplitudes are proportional to ϵ, I, as well as the squared rotation frequency $f_\star$:

$$h_0 = \frac{16\pi^2 G}{c^4}\frac{\epsilon\, I\, f_\star^2}{r}, \tag{17}$$

where r is the distance to the NS. Furthermore, the frequency of the GWs emanated depends on the mechanism that produces the mass quadrupole moment. In general, CGWs are generated at the first and second harmonic of the rotation frequency $f_\star$. We only consider the second harmonic ($f = 2f_\star$) in this work, because we find that the amplitude of the first harmonic is always lower than that of the second harmonic, which determines the detectability of the signal.

The corresponding GW polarizations are given by

$$h^+(t) = A^+\, h_0 \cos(2\pi f\, t + \varphi), \tag{18}$$

$$h^\times(t) = A^\times\, h_0 \sin(2\pi f\, t + \varphi), \tag{19}$$

where $A^+ = \sin\chi\frac{1+\cos^2\iota}{2}$ and $A^\times = \sin\chi\cos\iota$. Here, ι is the inclination angle between the rotation axis and the line of sight, χ is the angle between the rotation axis and the principal axis (called the wobble angle), and φ is a constant phase offset.

The measured GW strain at a detector depends on its response to the GWs. This response, characterized by the time-dependent antenna pattern functions $F^+(t)$ and $F^\times(t)$, depends on the relative orientation and location of the detector with respect to the location of the source:

$$h(t) = F^+(t)h^+(t) + F^\times(t)h^\times(t). \tag{20}$$

CGWs lensed by the galactic SMBH (modeled as a point-mass lens with mass M_L), will produce exactly two images with magnifications $\mu_\pm$ and time delay Δt. The resulting strain measured at the detector will therefore be a superposition between the two copies of CGWs:

$$h_{\rm tot}(t) = \sqrt{\mu^{\rm int}}[F^+(t)h^+(t) + F^\times(t)h^\times(t)]. \tag{21}$$

Here, $\mu^{\rm int}$ is an amplification factor that results from the interference of the two lensed signals, and is given by[7]

$$\mu^{\rm int} = |\mu_+| + |\mu_-| + 2\sqrt{|\mu_+\mu_-|}\cos(2\pi f\Delta t). \tag{22}$$

In order to assess the detectability of such signals, we evaluate an averaged S/N ρ (which depends on an averaged $h_{\rm tot}^2$), where the average is taken over the period of rotation of the NS (for $h^{+,\times}$), the sidereal day (for $F^{+,\times}$), as well as the inclination angle (ι), polarization angle (ψ), and wobble angle (χ):

$$\rho = \left[\frac{\langle((h^{\rm tot})^2\rangle(f)\,T_{\rm obs}}{S_n(f)}\right]^{1/2}. \tag{23}$$

Here, $S_n(f)$ is the detector's noise power spectral density (PSD), and $T_{\rm obs}$ is the observation time.

In order to estimate the detectability of strongly lensed NSs, we simulated populations of NSs within the lensing cone, distributed according to different models. We computed the lensing magnifications and time delays for each NS using Equations (5) and (7). We evaluate the single-detector S/N of the superposed images after accounting for interference (see Equations (21) and (22)), averaged over the rotation period of the NS, the wobble angle of the NS, the time-varying antenna patterns of the detector across a sidereal day, and the inclination angle of the rotation axis of the NS with respect to the line of sight. We set the sky location of the lensed sources to coincide with the location of SMBH (Sagittarius A*), which is a good approximation given that the Einstein angle extends to within an arcsecond centered at that location. We assume an ellipticity of $\epsilon = 10^{-7}$ and frequencies drawn from the frequency distribution of pulsars from the ATNF catalog (Manchester et al. 2005). The network S/N is the quadratic sum of the individual detector S/Ns (see Figure 3).

[7] Note that in addition to this amplification, lensing will add a constant phase $\varphi^{\rm int}$ to the signal that depends on the magnifications of the images and the time delay. This can be absorbed into the phase constant φ. However, proper motion of the source with respect to the optical axis will make $\mu^{\rm int}$ and $\varphi^{\rm int}$ time dependent, introducing amplitude and phase modulations in the lensed signal. This will help us distinguish lensed and unlensed signals; see Section 5.

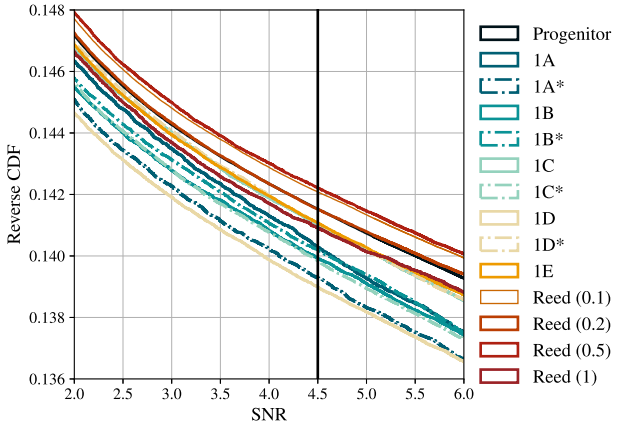

Figure 3. Cumulative distribution of the S/Ns of the lensed NSs for different spatial distributions (same as Figure 2). The S/N threshold of 4.5 corresponding to a false-alarm probability of 1% and false-dismissal probability of 10% using a single-template search is shown by the vertical line.

The fraction of detectable NSs within the Einstein angle is

$$N_{\theta_E}^{\rm det} = N_{\theta_E}\,\alpha(\rho_{\rm thresh}), \quad \alpha(\rho_{\rm thresh}) = \int_{\rho_{\rm thresh}}^{\infty} \frac{dP}{d\rho} d\rho, \qquad (24)$$

where the S/N distribution $dP/d\rho$ for each model is estimated from simulations. Figure 4 shows the distribution of detectable number of NSs within the Einstein cone. Depending on the model and the assumptions of the NS properties, the probability of detecting at least one strongly lensed NS is ∼2%–53%.[8] This is assuming an S/N threshold of 4.5 that corresponds to a false-alarm probability (FAP) of 1% and a false-dismissal probability (FDP) of 10% for a single-template search.

We also investigated the detection probability of lensed NSs in the fifth observing run (O5) of LIGO, Virgo, and KAGRA (Abbott et al. 2018) and find that the range of detection probabilities is ∼0%–15%.[9] However, a realistic search for such signals would require a bank of templates, since the intrinsic parameters of the NSs are not known a priori. Assuming a directed search toward the galactic center involving $\sim 10^{12}$ templates (Aasi et al. 2013), the S/N threshold corresponding to the FAP and FDP mentioned above, but now also accounting for the trials factor due to the template bank, becomes ≃9.6. With this threshold, the detection probability in O5 drops to ∼0%–2%. In 3G detectors, this probability continues to be nontrivial, with a range of ∼2%–51%. If we make a more pessimistic assumption of ellipticity $\epsilon = 10^{-8}$, LIGO–Virgo detectors are unlikely to detect any lensed signals. In 3G detectors the detection probability is ∼1%–36% for a single-template search and ∼0%–18% for a directed search involving 10^{12} templates. Smaller values of ϵ will reduce the detection probability further.

These estimates are consistent with the nondetection of CGWs by the directed searches toward the galactic center using LIGO–Virgo data from the third observing run (Abbott et al. 2022). Using the spatial and frequency distribution models that we employed to study the detectability of lensed signals, we estimate the detection probability of (all) CGWs to be ∼0%–2% with $\epsilon = 10^{-7}$ and a coherent integration time of 1 yr.[10] For the coherent integration times of a few hours employed in Abbott et al. (2022), the expected detection probability is almost zero.

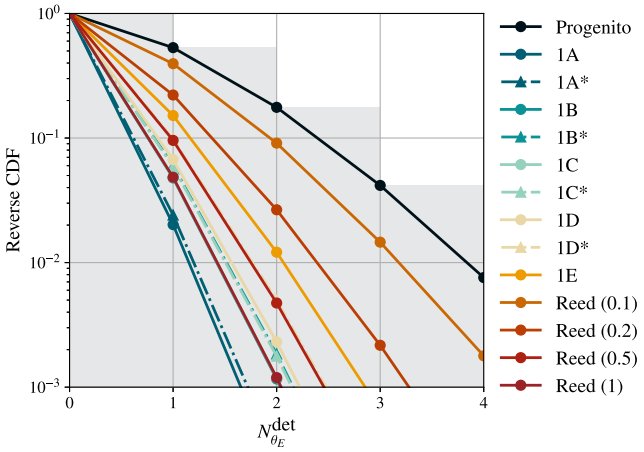

Figure 4. Cumulative distribution of the detectable number of strongly lensed events by 3G detectors with and S/N threshold of 4.5. The probability of at least one NS being inside the lensing cone, $P(N_{\theta_E}^{\rm det} \geqslant 1)$, is ∼2%–53%, depending on the model. The gray histogram shows the results computed using a simulation using the progenitor model, while the different lines are analytical calculations using Poisson distributions.

5. Discussion

In this Letter, we explored the possibility of detecting CGWs from spinning neutron stars strongly lensed by the galactic SMBH. Treating the SMBH as a point-mass lens, we consider a source to be lensed if it lies within the Einstein angle of the SMBH. To assess the prospects of detecting such lensed CGWs, we considered several spatial distributions of NSs presented in the literature. We find that up to 6 out of 10^9 NSs lie within the Einstein angle. Accounting for the lensing magnification and time delays as well as the resulting interference between the two images, we evaluate the detectability of such sources.

Unlike the lensing of GW transients such as compact binary coalescences, which gives temporally resolved copies of signals whose morphology can be compared to determine whether they are lensed, lensed CGWs would show up in the data as a single, interfered signal. If lensing introduces a constant time delay, the interfered signal would be indistinguishable from an unlensed CGW with the same amplitude, except for a constant phase shift. However, if the relative transverse motion between the NS and the lensing optical axis (axis connecting the Earth and the SMBH) is sufficiently large, the time delay Δt between the lensed copies of the CGW itself becomes a function of time. This will result in the modulation of the amplitude and phase of the lensed CGW signals, rendering them identifiable.

Generically, we expect some relative motion between the NS and the optical axis. This could be due to the proper motion of the NS in the galaxy (e.g., due to the natal kicks;

[8] We assume a three-detector network consisting of two CE detectors and one ET. The expected PSDs are generated from the "optimal" curves presented in Figure 2 of Hall & Evans (2019).

[9] We assume a five-detector network involving three LIGO detectors (including LIGO-India), Virgo, and KAGRA. The expected PSDs are generated using ALIGOAPLUSDESIGNSENSITIVITYT1800042, ADVVIRGO, and KAGRALATESENSITIVITYT1600593 functions of the PyCBC PSD package (Nitz et al. 2022).

[10] Here we assume that the search is directed toward NSs located in a cone that has its apex on the Earth and has a base radius equal to the Einstein radius of the SMBH for a source at $D_{SL} = 15$ kpc.

$v \sim 100\ \mathrm{km\ s^{-1}}$), due to the motion of the Earth around the Sun ($v \sim 30\ \mathrm{km\ s^{-1}}$), or due to the differential motion of the solar system in the galactic potential ($v \sim 10\ \mathrm{km\ s^{-1}}$). A simple, back-of-the envelope calculation can give an estimate of the degree of this modulation. From Equation (7), the accumulated change in the lensing time delay over an observational time T can be estimated as $\simeq 2\frac{D_L D_S}{c\ D_{SL}}\theta_E\ \frac{d\beta}{dt}\ T \simeq 2\frac{D_L}{c\ D_{SL}}\theta_E\ v\ T$. This can cause several modulation cycles in the amplitude and phase of the CGW signal over the course of 1 yr, helping us to identify lensed signals.

Lensed CGWs, if detected, would enable unique probes of astrophysics and gravity. For example, the lensing time delay and hence the amplitude and phase modulation of the lensed CGW signal depends on the mass of the SMBH. Such an observation would be a unique new way of measuring the mass of the galactic SMBH. In addition, compact objects and stars in the galactic center could produce additional microlensing effects on the GW signal, which are potentially measurable (Liao et al. 2019; Marchant et al. 2020; Suvorov 2022). This would be a powerful means of probing the astrophysical environment of the galactic center. Unlike electromagnetic radiation GWs do not suffer from extinction and can potentially provide an uncontaminated picture. Lensed CGW signals can, in principle, contain signatures of additional properties of the SMBH, such as its spin angular momentum (Gralla & Lupsasca 2020), and more speculatively, other possible "hairs" (Islam & Ghosh 2021). They will also allow us to measure the proper motion of the NS. Lensing of CGWs harbors a rich and complex phenomenology, which we plan to explore in upcoming work.

We thank David Keitel for reviewing the manuscript and providing useful comments. We acknowledge the support of the Department of Atomic Energy, Government of India, under project No. RTI4001. S.J.K.'s work was supported by a grant from the Simons Foundation (677895, R.G.) to the International Centre for Theoretical Sciences, Tata Institute of Fundamental Research (ICTS-TIFR). P.A.'s research was supported by the Canadian Institute for Advanced Research through the CIFAR Azrieli Global Scholars program. Computations were performed with the aid of the Alice computing cluster at ICTS-TIFR.

ORCID iDs

Soummyadip Basak https://orcid.org/0000-0002-1824-3292
Aditya Kumar Sharma https://orcid.org/0000-0003-0067-346X
Shasvath J. Kapadia https://orcid.org/0000-0001-5318-1253
Parameswaran Ajith https://orcid.org/0000-0001-7519-2439

References

Aasi, J., Abadie, J., Abbott, B. P., et al. 2013, PhRvD, 88, 102002
Aasi, J., Abadie, J., Abbott, B. P., et al. 2015, CQGra, 32, 074001
Abbott, B. P., Abbott, R., Abbott, T. D., et al. 2017a, PhRvL, 119, 161101
Abbott, B. P., Abbott, R., Abbott, T. D., et al. 2017b, Natur, 551, 85
Abbott, B. P., Abbott, R., Abbott, T. D., et al. 2018, LRR, 21, 3
Abbott, B. P., Abbott, R., Abbott, T. D., et al. 2019a, PhRvX, 9, 031040
Abbott, B. P., Abbott, R., Abbott, T. D., et al. 2019b, PhRvD, 100, 024004
Abbott, B. P., Abbott, R., Abbott, T. D., et al. 2020, ApJL, 892, L3
Abbott, B. P., Abbott, R., Abbott, T. D., et al. 2020, LRR, 23
Abbott, R., Abbott, T. D., Abraham, S., et al. 2020a, PhRvX, 11, 021053
Abbott, R., Abbott, T. D., Abraham, S., et al. 2020b, PhRvD, 103, 122002
Abbott, R., Abbott, T., Acernese, F., et al. 2021, arXiv:2111.03606
Abbott, R., Abbott, T. D., Abraham, S., et al. 2021a, ApJL, 915, L5
Abbott, R., Abbott, T. D., Abraham, S., et al. 2021b, ApJL, 913, L7
Abbott, R., Abbott, T. D., Abraham, S., et al. 2021c, ApJ, 923, 14
Abbott, R., Abbott, T. D., Abraham, S., et al. 2021d, PhRvD, 103, 064017
Abbott, R., Abbott, T. D., Abraham, S., et al. 2022, PhRvD, 106, 042003
Acernese, F., Agathos, M., Agatsuma, K., et al. 2015, CQGra, 32, 024001
Akutsu, T., Ando, M., Arai, K., et al. 2021, PTEP, 2021, 05A101
Andersson, N. 2019, Gravitational-wave Astronomy: Exploring the Dark Side of the Universe (Oxford: Oxford Univ. Press)
Basak, S., Ganguly, A., Haris, K., et al. 2022, ApJL, 926, L28
Bonazzola, S., & Gourgoulhon, E. 1996, A&A, 312, 675
Dai, L., Zackay, B., Venumadhav, T., Roulet, J., & Zaldarriaga, M. 2020, arXiv:2007.12709
Dodelson, S. 2017, Gravitational Lensing (Cambridge: Cambridge Univ. Press)
Evans, M., Adhikari, R. X., Afle, C., et al. 2021, arXiv:2109.09882
Ezquiaga, J. M., & Zumalacárregui, M. 2020, PhRvD, 102, 124048
Fan, X.-L., Liao, K., Biesiada, M., Piorkowska-Kurpas, A., & Zhu, Z.-H. 2017, PhRvL, 118, 091102
Ghez, A. M., Duchêne, G., Matthews, K., et al. 2003, ApJL, 586, L127
Goyal, S., Haris, K., Mehta, A. K., & Ajith, P. 2021, PhRvD, 103, 024038
Gralla, S. E., & Lupsasca, A. 2020, PhRv, 101, 044031
Hall, E. D., & Evans, M. 2019, CQGra, 36, 225002
Hannuksela, O. A., Collett, T. E., Çalşkan, M., & Li, T. G. F. 2020, MNRAS, 498, 3395
Islam, S. U., & Ghosh, S. G. 2021, PhRv, 103, 124052
Jaranowski, P., Królak, A., & Schutz, B. F. 1998, PhRv, 58, 063001
Jung, S., & Shin, C. S. 2019, PhRvL, 122, 041103
Liao, K., Biesiada, M., & Fan, X.-L. 2019, ApJ, 875, 139
Manchester, R. N., Hobbs, G. B., Teoh, A., & Hobbs, M. 2005, AJ, 129, 1993
Marchant, P., Breivik, K., Berry, C. P. L., Mandel, I., & Larson, S. L. 2020, PhRvD, 101, 024039
Ng, K. K. Y., Wong, K. W. K., Broadhurst, T., & Li, T. G. F. 2018, PhRv, 97, 023012
Nitz, A., Harry, I., & Brown, D. 2022, gwastro/pycbc: v2.0.5 release of PyCBC, Zenodo, doi:10.5281/zenodo.6912865
Paczynski, B. 1990, ApJ, 348, 485
Punturo, M., Abernathy, M., Acernese, F., et al. 2010, CQGra, 27, 084007
Reed, B. T., Deibel, A., & Horowitz, C. J. 2021, ApJ, 921, 89
Sartore, N., Ripamonti, E., Treves, A., & Turolla, R. 2010, A&A, 510, A23
Schödel, R., Ott, T., Genzel, R., et al. 2002, Natur, 419, 694
Smith, G. P., Bianconi, M., Jauzac, M., et al. 2019, MNRAS, 485, 5180
Suvorov, A. G. 2022, ApJ, 930, 13
Treves, A., Turolla, R., Zane, S., & Colpi, M. 2000, PASP, 112, 297
Urrutia, J., & Vaskonen, V. 2022, MNRAS, 509, 135